DOI: 10.48011/sbse.v1i1.2416

Control and Application of Single-phase PWM Rectifier in Aircraft Electric Systems

Bruno Valverde and José Antenor Pomilio

** Department of Systems and Energy (DSE), University of Campinas (UNICAMP)*
Campinas, Brazil (brnovalverde@gmail.com, antenor@unicamp.br)

Abstract: This work studies the use of single-phase high power factor PWM rectifiers in aircrafts with variable frequency (360 to 800 Hz) power generation. It also presents design guidelines for input and output filters, and discusses the modeling and design of the voltage and current controllers. A 1 kW system is simulated considering a variable frequency grid, verifying the compliance with the aircraft power quality standards. Experimental results from a prototype allows to verify the design procedures.

Resumo: Este trabalho estuda o uso de retificadores PWM de alto fator de potência em aeronaves com barramento CA de frequência variável (360 a 800 Hz). Ele também apresenta diretrizes de projeto para filtros de entrada e saída, e discute a modelagem e o projeto dos controladores de tensão e corrente. Um sistema de 1 kW é simulado considerando uma rede de frequência variável, verificando a conformidade com os padrões de qualidade de energia da aeronave. Os resultados experimentais de um protótipo permitem verificar os procedimentos de design.

Keywords: More Electric Aircraft; PWM rectifier; Power Quality; Airplane grid; Power Electronics

Palavras-chaves: Aeronaves mais elétricas; Retificador MLP; Qualidade de Energia Elétrica; Rede elétrica embarcada em aviões; Eletrônica de Potência

1. INTRODUCTION

Air transportation presents a noteworthy growing during XX and beginning of XXI centuries (World Bank, 2017). Part of such development is a result of the technological improvements, providing cost reduction and offer expansion (Hartmann, 2011).

Conventional systems, composed by a combination of pneumatic, hydraulic, mechanical and electrical devices, are being replaced by electrical and electronic systems (Eid, 2009), the so called More Electrical Aircraft (MEA) movement (Quigley, 1993).

The MEA concept aims to transform all the aircraft systems into electrical/electronic solutions. This allows higher airplane reliability and control efficacy, granting more safety, and economic benefits. Since the electrical systems are lighter than the conventional solutions, the aircraft consumes less fuel in the flight. However, despite the many benefits, the full implementation of MEA concept presents many challenges. It's necessary to guarantee all the electrical and electronics devices operate in all conditions, including fault situations (Todd, 2011).

Therefore, analysis and evaluations regarding electrical power quality become mandatory (Alves, 2016). Standards, such MIL-STD-704F (USA DoD, 2004), is related to the voltage behavior of airplane embedded grid. The RTCA DO-160G (RTCA, 2010) determines the expected behavior of the electric equipment installed in the aircraft. In this sense, it regulates the current behavior.

The traditional power generation in aircrafts uses the variable speed, constant frequency procedure. Between the turbine (the primary power source) and the generator there's an automatic gear box aimed to maintain constant the output speed, allowing the generator to produce power at 400 Hz. One of the goals of the MEA is to reduce the airplane weight. By connecting the generator directly to the turbine, the heavy gear box is eliminated. However, the AC power generation operates with variable frequency (between 360 and 800 Hz). This implies the design of the electric and electronic loads must consider the AC input voltage with such characteristic.

Besides the variable frequency AC primary bus, the airplane electric network also presents DC buses. The low voltage DC bus (28 V) feeds the so called "avionics", the electronic devices and apparatus necessary for guaranteeing the flying conditions. The high voltage DC bus (single 270 V or symmetrical +/- 270 V) typically feeds high power loads, as inverters controlling AC motors and actuators (Abdel-Fadil, 2018). The power converter of higher capability in this grid is the rectifier that creates the high-voltage DC bus that feeds most of the final application converters.

The RTCA DO-160G defines, among other specifications, the current harmonic content, as shown in Tables 1 and 2. Note in Table 1 that the limit for 5th and 7th harmonics is 2% of the fundamental. Such restriction, in practice, eliminates the use of six-pulse diode rectifiers. A possible solution is the 12 pulse rectifier (Vitoi, 2017). Such topology is suitable for constant frequency (400 Hz) systems because it's easy to design the input (AC current harmonic content) and output (DC voltage

ripple) filters, which are necessary for the compliance with the standards. With this converter the DC voltage isn't controlled.

Table 1. Current harmonic limits for balanced three-phase equipment (RTCA, 2010)

Harmonic order	Limits
3rd, 5th, 7th	$I_3 = I_5 = I_7 = 0.02I_1$
Odd triplen harmonics (9, 15, … 39)	$I_h = 0.1I_1/h$
11th	$I_{11}=0.1I_1$
13th	$I_{13}=0.08I_1$
Odd non triplen harmonics 17, 19	$I_{17} = I_{19} = 0.04I_1$
Odd non triplen harmonics 23, 25	$I_{23} = I_{25} = 0.03I_1$
Odd non triplen harmonics 29, 31, 35, 37	$I_h = 0.3I_1/h$
Even harmonics 2 and 4	$I_h = 0.01I_1/h$
Even harmonics > 4 (h=6, 8, ... 40)	$I_h = 0.0025I_1$

Table 2. Current harmonic limits for balanced single-phase equipment

Harmonic order	Limits
Odd non triplen harmonics (h=5, 7, 11, . . . 37)	$I_h = 0.3I_1/h$
Odd triplen harmonics (h=3, 9,...39)	$I_{17}=I_{19}=0.15I_1$/h
Even harmonics 2 and 4	$I_h = 0.01I_1/h$
Even harmonics > 4 (h = 6, 8, . . . , 40)	$I_h = 0.0025I_1$

I_1 = maximum fundamental current of the equipment that is measured during the maximum steady-state power demand operating mode condition, at a single test frequency
h = order of harmonic
I_h = maximum harmonic current of order h obtained for all normal steady state modes of operation.

In case of double DC bus, the 12 pulse rectifier can present problems since the effective 5th and 7th harmonic cancelation occurs only in case of balanced loads, what isn't possible to guarantee. In case of unbalanced loads it's necessary to provide an additional converter in order to equalize the currents or to cancel the harmonics at the AC bus.

Alternatively, active PWM rectifiers (single- or three-phase bridges, Vienna Rectifiers, etc.) converters have been studied and compared regarding their volume, efficiency and weight in MEA systems (Gong, 2005). The PWM rectifier allows low input current distortion as well as the output voltage regulation. Double DC bus is possible with three-phase, four-wire converters (Bueno, 2018).

Considering reliability issues, it is valid to assume that a modular conversion system (multiple converters in parallel operation) can be an advantage under fault conditions (Bueno, 2019). This work investigates a PWM single-phase rectifier in a variable frequency network. The complete rectification module would be composed by three single-phase rectifiers, scaled to 1/3 of the total power. In case of fail of the converter, they should be design to operate in overload.

Section 2 describes the circuit topology and passive component dimensioning. Section 3 describes the control strategy and the controllers design. In section 4 is shown the simulation results, analysing the compliance with the standards. The section 5 is reserved for experimental results. In section 6, the conclusions are listed.

2. TOPOLOGY

The single-phase PWM rectifier topology is shown in Fig. 1. From the command of S1 to S4 switches, the inductor is energized and its energy is transferred to the DC link capacitor (Barbi, 2015). This converter has a boost behaviour, which means the output voltage is higher than the input peak voltage. The three level modulation is preferred because it allows a lower input inductance.

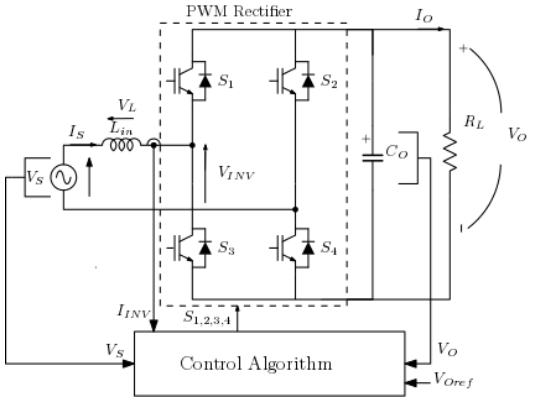

Fig. 1 Single-phase PWM rectifier.

The input circuit considers the inductance of grid cabling between the generator and the point of common coupling (PCC), where the rectifier is connected. At the PCC the voltage must comply with the MIL-STD-704F. Usually this regulation is provided by the excitation of the synchronous generator. The PWM rectifier input current must comply with the RTCA DO-160G.

The effects of the high frequency commutation propagate through the feeder, affecting the grid voltage, causing power quality problems on the PCC. A simple first order inductive filter isn't enough to guarantee the voltage quality, because it'd be necessary a too high inductance, limiting the power conversion capability. For that, it's used a LCL filter. The converter, including filters and control blocks is in Fig. 2.

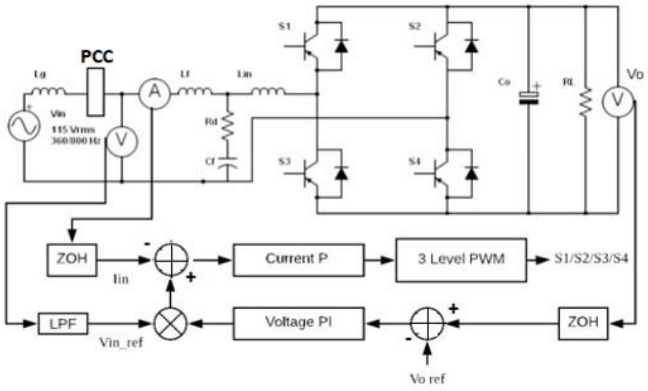

Fig. 2 PWM Rectifier with LCL filter and control blocks.

2.1 Input inductance, filtering and output capacitance modelling

As the converter presents a step-up characteristic, the inductance value calculation uses the same procedure of a boost converter, according to (1).

$$L_{in} = \frac{0.25\,V_0}{2\Delta I_L f_s} \quad (1)$$

V_o is the output voltage, ΔI_L is the maximum current ripple and f_s is the switching frequency. The input inductance value is subjected to some additional restrictions. Firstly, in a single-phase rectifier, the voltage produced at the rectifier input must compensate the voltage drop of the inductance V_L, so the relation between source voltage and current is preserved, as shown in Fig. 3 (Pomilio, 2018).

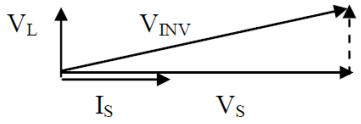

Fig. 3 Phasor representation of source (Vs), converter (V_{INV}) and inductor (V_L) voltages and input current.

Considering the phase grid RMS voltage (115 V) and DC bus voltage (270 V), V_L is given from (2). At the maximum frequency, the maximum inductance is given by (3).

$$\dot{Vinv} = \dot{VL} + \dot{Vs} \quad (2)$$

$$\omega L_{fmax} = |X_{fMAX}| = \frac{|V_{inv}|}{|\dot{I}_{max}|} \quad (3)$$

For getting unity power factor, and considering that the maximum input current is a function of the power at the minimum value of voltage grid (108 V), the maximum input inductance is:

$$|\dot{I}_{max}| = \frac{|V_{inv}|}{|\dot{Vsmin}|} \quad (4)$$

$$L_{max} = \frac{(\sqrt{(Vinv_{max})^2 - (V_s)^2})|\dot{Vsmin}|}{2\pi f_{in} P_{max}} \quad (5)$$

An inductance value above the limit will not permit the energy transferring between source to the load, still maintaining the power factor close to unity, as necessary.

Secondly, it also need to verify the input current spectrum compliance with the RTCA DO-160G. For example, for a 20 kHz switching frequency, in the worst case (with 800 Hz grid frequency), the switching frequency component coincides in the 25th harmonic. Following RTCA DO-160G for 25th harmonic, and considering the fundamental current as input power (P_{in}) divided by input voltage, the ripple current is given by (6). Replacing (6) in (1) it's possible to have the minimum inductance for complying with the standard (7).

$$I_{25\,peak} = \frac{0{,}3P_{in}\sqrt{2}}{25\,V_{in}} \quad (6)$$

$$L_{\min 25} = \frac{0{,}25\,V_0\,25\,V_{in}}{2{*}0{,}3P_{in}\sqrt{2}{*}f_s} \quad (7)$$

Plotting the power as a function of the maximum inductance, considering the maximum frequency (800 Hz), it can be observed the inductance value decreases as the power increases. Plotting the converter's minimum inductance value working in 20 kHz and at 31.2 kHz (that is the switching frequency that correspond to the 39th harmonic of 800 Hz), it's not possible to obtain a compromise between an inductance that attends the harmonics standard and can operate under variable frequency.

Since the use a simple L filter may be not feasible, a high order input filter must allow using a lower inductance while reducing the high frequency propagation. For a LCL input filter, following the methodology given in Barbi (2015), at 35 kHz switching frequency, and considering 5% of current ripple, the inductor value is given by (8). For 1 kW, the inductance is 1,4 mH. Fig. 4 shows this value is below the inductance value for transferring 1 kW at 800 Hz.

$$L_{in\_35kHz} = \frac{0{,}25\,V_0\,V_{in}}{2{*}0{,}05P_{in}\sqrt{2}{*}35kHz} \quad (8)$$

Since L_{IN} is known, the LCL filter design (Liserre, 2005) considers a resonance (cut-off) frequency of 4985 Hz (14 times the lowest input frequency, 360 Hz), an attenuation factor of 0.38 and absorbed reactive power 0.017, the resulting values are shown in Table 3. For this R_d value, the filter losses will be 12,1 W, around 1,2% of input power. The damping resistance was placed in series with a capacitor five times larger than C_f, as shown in Fig. 5, to attenuate the resonance of the LCL filter.

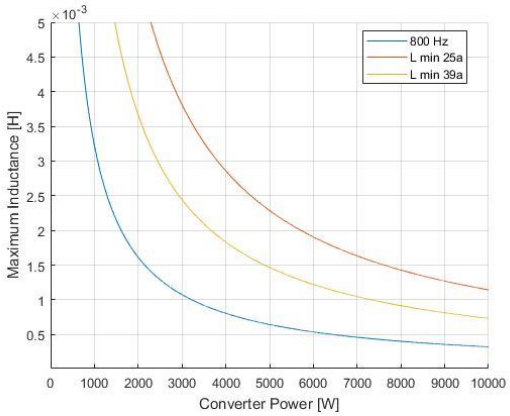

Fig. 4 Output power vs. maximum input inductance @ 800 Hz (Blue), L_{min} for 20 kHz (Red), for 31.2 kHz (Yellow), for processing 1kW.

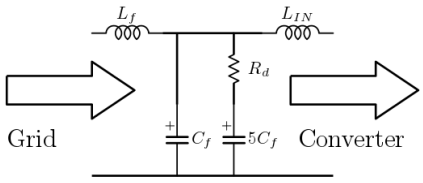

Fig. 5. LCL filter with RC damping branch.

Table 3. Passive component values of LCL filter

Components	Values
L_{IN}	1,4 mH
C_f	560 nF
L_f (includes grid inductance)	63,8 µH
R_d	4,7 Ω

The effect of the grid inductance L_g, is included in the L_f value. It is worth noting that the sum of total inductances does not surpass the maximum inductance limit for the worst case of energy transferring shown in Fig. 4.

The value of the output (DC) capacitor is given by (9). P_o is output power; f_{in} is the AC grid frequency and ΔV_{cpp} is the peak to peak DC voltage ripple. For 1 kW, 360 Hz (worst case for capacitance) and a 0.3% ripple (compliance with MIL-STD-704F), the capacitance value is 970 µF.

$$C_O = \frac{P_O}{4\pi f_{in} V_O \Delta V_{cpp}} \tag{9}$$

3. CONTROL LOOPS

The PWM rectifier control strategy is the so called resistive load synthesis, in which the unity power factor is obtained by using the input voltage shape to give the same waveform to the input current. For that, it is necessary to have both, current and DC voltage controllers.

For the controllers design, it was considered P regulator for the current and a PI regulator for voltage loop, according to Buso (2015). In practice, both control loops are decoupled, since the first one is much slower than the second one. The reason of using a P controller is that the control signal does not require a null steady state error.

For the current loop, the plant transfer function is (10). The total input inductance (L_{in}) is the sum of L_{IN} and L_f, which includes the grid inductance. LCL filter has an inductive behaviour on the fundamental frequency, so only the inductors are considered, neglecting the capacitor effect. In (11), it is considered the delay caused by the PWM using the Padé's approximation, where T_s is the switching period and c_{pk} is the peak value of the PWM carrier. It is also considered the current sensor gain G_{MI}. Fig. 6 shows the block diagram for current controller.

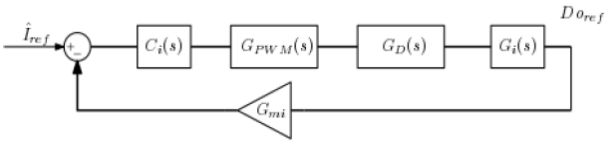

Fig. 6 Current Control Loop.

$$G_I(s) = \frac{V_O}{sL_{in}} \tag{10}$$

$$G_{PWM}(s) = \frac{1}{c_{pk}} \frac{1 - {T_s}/{4}s}{1 + {T_s}/{4}s} \tag{11}$$

Calculating the open loop transfer function (12), and the open loop gain module as 1 at the desired cut off frequency ω_{ci}, it is possible to obtain the P regulator gain (Buso, 2015).

$$G_{OLI}(s)|_{s=jwcli} \cong |1| =$$

$$= (K_P) * \frac{1}{c_{pk}} \frac{1 - {T_s}/{4}s}{1 + {T_s}/{4}s} * \frac{V_O}{sL_{in}} * G_{MI} \tag{12}$$

Considering the plant's transfer function real part as an approximation for the proportional gain K_p, the respective gain are in (13). For a cut-off frequency 8 times lower than the switching frequency (4,32 kHz), output voltage V_o = 270 V, c_{pk} = 1, G_{MI} = 0.01 and inductance 1,4 mH according to (8), results in K_p = 16.4.

$$K_P = \frac{L_{in}\omega_{Cli} c_{pk}}{V_O G_{MI}} \tag{13}$$

The DC voltage control block diagram is shown in Fig. 7. From the power balance it's possible to obtain the respective transfer function, given by (14). R_L is the equivalent load resistance, equal to 72.9 Ω (for 1 kW @ 270 V).

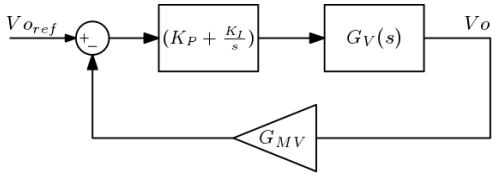

Fig. 7 Voltage control loop.

$$G_V(s) = \frac{R_L V_{in}^2}{2V_0} \frac{V_O}{1 + s{R_L C_0}/{2}} G_{Mv} \tag{14}$$

Following the previous methodology, the DC voltage controller gains are calculated, according with (15) and (16). The phase margin is 62° at the cut-off frequency of 300 Hz. The voltage loop cut-off frequency is established for transient response for load variations, according to MIL-STD-704F specifications. The load R_L was considered 10 times higher (729 Ω) in (15) and (16). The resulting gains are Kp = $3.73*10^1$ and Ki = $3.76*10^4$.

$$K_P = \frac{2V_0}{G_{MV} R_L V_{in}^2} \left(1 + \frac{\omega_{CLV} R_L C_0}{2}\right) \tag{15}$$

$$K_I = \frac{K_P \omega_{CLV}}{\tan\left[-90 + \varphi_{mar} + \tan^{-1}\left(\omega_{CLV} {R_L C_0}/{2}\right)\right]} \tag{16}$$

4. SIMULATION RESULTS

PLECS® simulations, shown in Fig. 8, include additional components, as the output capacitors series resistance, and input and grid inductances. At the measuring point, a low pass filter at 20 kHz is necessary to avoid the contamination of the reference voltage waveform by the switching effect. The values are in Table 4. The voltage and current waveforms at 800 Hz shown in Fig. 9, indicates both have the same shape, resulting in a very high power factor.

Table 4. Parameter values of simulated system.

Parameters	Values
Po	1 kW
Co	970 µF
R_{se}	11 mΩ
L_{in}	1,4 mH
Fs	35 kHz
C_{hf}	10 µF
C_f	560 nF
L_g	63,8 µH
R_{lg}	3.81 mΩ
V_{in}	115 V_{rms}

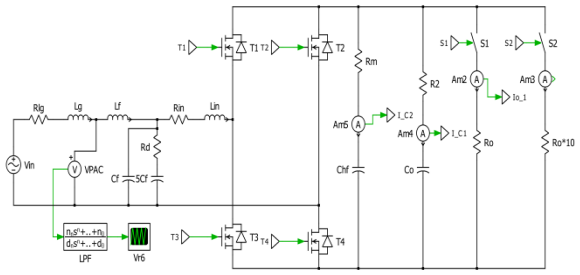

Fig. 8 Simulated circuit with elements of grid inductance, LCL filter and input low pass filter.

The total distortion factor (18) according with the MIL-STD-704F, is 0,59%, lower than the 5% allowed value. Also regarding the current harmonics, they comply with the limits.

$$FD = \frac{V_{RMS}}{V_1} - 1 \tag{18}$$

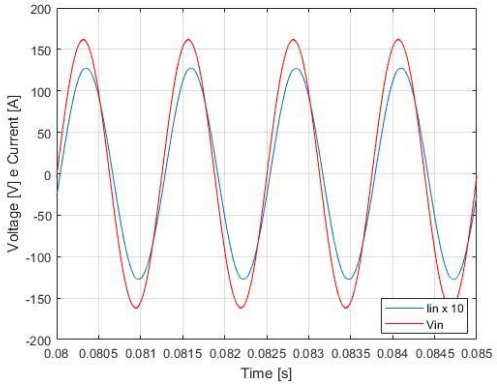

Fig. 9 Voltage and current waveform at 800 Hz.

Regarding the voltage at the PCC, Fig. 10 shows the spectra for different switching frequencies, compared to the MIL-STD-704F limits. Also for the AC voltage, the operation of the PWM rectifier allows the compliance with the standard.

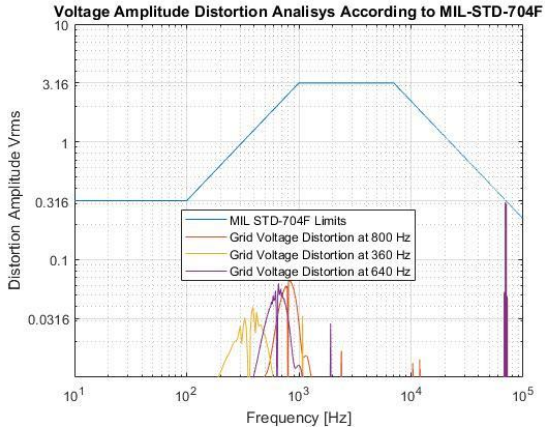

Fig. 10: Maximum distortion limit in voltage input (blue) and found in simulation for different frequencies: 800 Hz (red), 360 Hz (yellow) and 640 Hz (purple).

The control strategy efficacy for getting unity power factor was analysed at different frequencies (360, 640 and 800 Hz). As expected, the current waveform follows the voltage waveform in all situations, as shown in Fig. 11.

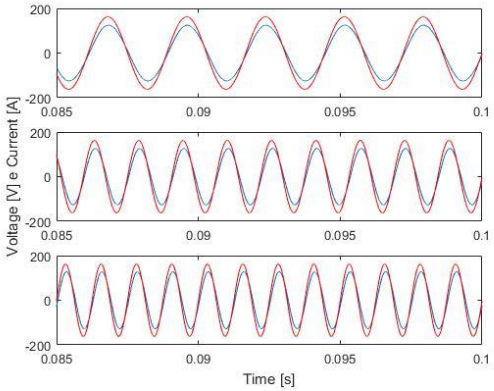

Fig. 11 Voltage and current waveforms in 360 Hz (above), 640 Hz (middle) and 800 Hz (below).

It was also verified the output voltage transitory with frequency rising and, simultaneously, load variation. At 0.1 s the load changes from 100% to 10%. At 0.2 s occurs the opposite variation (Fig. 12). The DC link operates according with the standard in both situations. The output voltage ripple is lowered according AC frequency rise and it's also complying with the limit of 6 V (USA DoD, 2004).

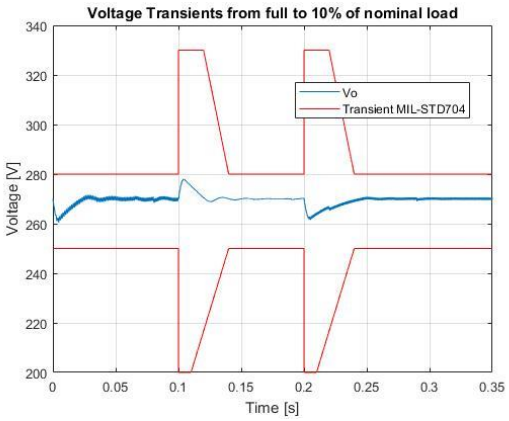

Fig. 12: Output voltage transient with frequency sweep and load variation (blue) and envelope of MIL-STD-704F for output voltage transients (red).

5. EXPERIMENTAL RESULTS

A 1 kW prototype, switching at 35 kHz, and operating with input variable frequency was built for validation of the results. The controller gains were recalculated and the proper LCL filter was also built. For the experimental design, a F28335 DSP of Texas Instruments® was used for current and voltage digital control, as also for AD Conversion.

The operating system in 360 Hz with 1 kW (86 Ω load) can be seen in Fig. 13. It's worth noting the current follows the voltage shape and also the output voltage value, 270 V_{DC}, is achieved. The measured power factor is 0.99. The harmonic content complies with RTCA (2010). The output voltage transient can be seen in Fig. 14. For the test the load was changed from 156 to 86 Ω. The DC voltage controller works properly, regulating the output voltage.

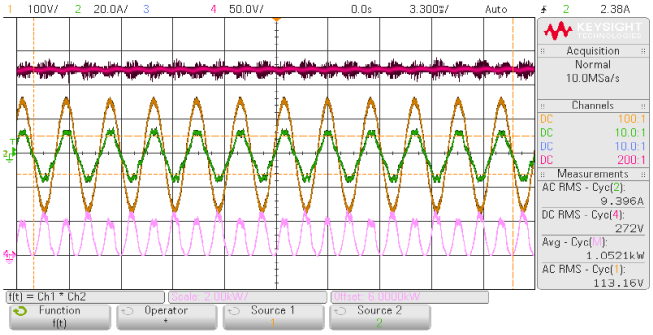

Fig. 13 Prototype results for 1kVA @ 360Hz frequency: grid voltage (yellow); grid current (green); Voltage output (purple) and input power calculation (pink).

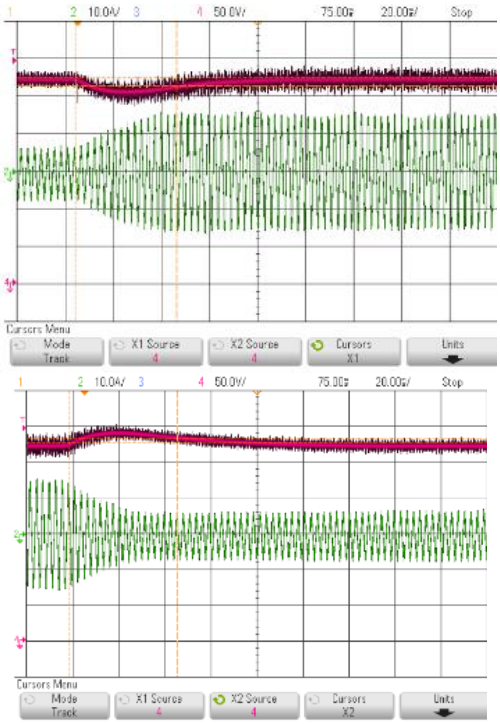

Fig. 14 Transient results for 1kVA @ 360Hz frequency: Voltage output (purple) and input current (green).

6. CONCLUSIONS

According to the results, the single-phase PWM rectifier and the respective controllers can properly work in variable frequency aircraft electrical systems. It was possible to identify important restrictions, as the necessity of a high order AC input filter in order to allow having the rated power and getting compliance with the standards regarding current and voltage distortion. A procedure for designing the controllers for regulating the output DC voltage and the input current was developed and its effectiveness shown for frequency sweep and load variation. With experimental results, it was possible to verify the circuit implementation.

AKNOWLEGMENTS

The authors want to thank São Paulo Research Foundation, FAPESP, grant #2017-05565-7, and Brazilian National Council for Scientific and Technological Development, CNPq, grant 401216/2016-0.

REFERENCES

Abdel-Fadil, R., Eid, A., and Abdel-Salam, M., Electrical Distribution Power Systems of Modern Civil Aircrafts. International Conference on Energy Systems and Technologies, in *2nd International Conference on Energy Systems and Technologies*, Cairo, Egypt, 2018.

Alves, J., de Figueiredo, J.P., Malizia, I., and Pomilio, J., Analysis and tests of Power Quality in aviation environment, *17th IEEE International Conference on Harmonics and Quality of Power* (ICHQP), Belo Horizonte, Brazil, 2016.

Barbi, I., "*Conversores Monofásicos Bidirecionais com Correção Ativa do Fator de Potência*", Florianopolis, Brazil: Federal University of Santa Catarina, 2015.

Buso, S. and Mattavelli, P., *Digital Control in Power Electronics*. [S.l.]: Morgan & Claypool, 2015.

Bueno, A.G.; Pomilio, J.A.; Balancing Voltage in the DC Bus with Split Capacitors in Three-Phase Four-Wire PWM Boost Rectifier, *13th IEEE International Conf. on Industry Applications*, São Paulo, Brasil 2018.

Bueno, A.G., and Pomilio, J., Three-phase, four-wire PWM rectifier applied to variable frequency AC systems in airplane electric grid under fault conditions, *5th IEEE Southern Power Electronics Conference & 15º Congresso Brasileiro de Eletrônica de Potência*, Santos, Brazil, 2019.

Eid, A., Abdel-Salam, M., El-Kishky, H., and El-Mohandes, T., "Simulation and transient analysis of conventional and advanced aircraft electric power systems with harmonics mitigation", *Electric Power Systems Research*, vol. 79, no. 4, pp. 660-668, 2009.

Gong, G., *et alli*, Comparative Evaluation of Three-Phase High-Power-Factor AC–DC Converter Concepts for Application in Future More Electric Aircraft, *IEEE Transactions on Industrial Electronics*, vol. 52, no. 3, pp. 727-737, 2005.

Hartmann, M. *Ultra-Compact and Ultra-Efficient Three-Phase PWM Rectifier Systems for More Electric Aircraft.* PhD Thesis, ETH Zurich, Switzerland, 2011.

Liserre, M., Blaabjerg, F., and Hansen, S., Design and Control of an LCL-Filter-Based Three-Phase Active Rectifier, *IEEE Transactions on Industry Applications*, vol. 41, no. 5, pp. 1281-1291, 2005.

Pomilio, J.A., *Pré-Reguladores de Fator de Potência* (in Portuguese). http://www.fee.unicamp.br/dse/antenor/pfp. Access on June 15, 2018.

Quigley, R., More Electric Aircraft, *Proceedings Eighth Annual Applied Power Electronics Conference* and Exposition, 1993.

RTCA - RADIO TECHNICAL COMISSION FOR AERONAUTICS. DO160G: Environmental Conditions and Test Procedures for Airborne Equipment. 2010.

Todd, R. and Forsyth, A., DC-bus power quality for aircraft power systems during generator fault conditions, *IET Electrical Systems in Transportation*, vol. 1, no. 3, p. 126, 2011.

USA DoD - DEPARTMENT OF DEFENSE. MIL-STD-704F. Aircraft Electric Power Characteristics. Department of Defense Interface Standard. 2004. 38 p.

Vitoi, L., Pomilio, J., and Brandao, D., Analysis of 12-pulse diode rectifier operating in aircraft systems with variable frequency, *3rd IEEE Southern Power Electronics Conference*, Puerto Varas, Chile, 2017.

World Bank. (2017). *Air transport, passengers carried* |Data Retrieved June 8, 2018, from: http://data.worldbank.org/indicator/IS.AIR.PSGR?end=2015&start=1970&view=chart